Science Arena Publications
Specialty Journal of Engineering and Applied Science
ISSN: 2520-5943
Available online at www.sciarena.com
2020, Vol, 5 (2): 49-59

On the Investigation of the Optimal Position of the Vane on Free Convection Heat Transfer around the Cylinder near Two Adiabatic Walls

Seyyed Reza Fattahi Kalajahi

MSc in Mechanical Engineering (Energy Conversion), Jolfa Interntional Branch, Islamic Azad University, Jolfa, Iran.

Abstract: *Considering the global energy crisis since the last two centuries, heat transfer and improving its process and reducing the losses have become the most important issues of our time. Therefore, improving the heat transfer functioning from the viewpoint of reducing manufacturing costs by using fewer materials or reducing operating costs by reducing energy losses, is of economic and ecological importance. For some economic and ecological reasons, it is important to achieve effective heat transfer in many industries involving a transfer of heat from gas to gas or from gas to liquid. Hence, free convection heat transfer and enhanced thermal efficiency have attracted the attention of many researchers in recent years. The present work studies free convection heat transfer around a cylinder near the adiabatic wall. Modeling results were well consistent with the experimental results, indicating the accuracy of the present modeling process. To optimize heat transfer in the cylinder, vanes of different shapes were placed in the flow path. The shape, size and position of these vanes and their thermal efficiency were other parameters studied in this dissertation.*

Keywords: *free convection heat transfer, vane, Nusselt number, thermal efficiency*

INTRODUCTION

The important role of heat transfer and fluid flow is always seen in our lives and in many practical respects (Gebhart et al., 1988; Holman Jack et al., 1992; Park and Chung, 1999; Park and Jung, 2001). Almost all power generation methods including fluid flow and heat transfer are focused attention as the main processes used in important sectors including chemical and metallurgical industries to be applied in furnaces, heat converters, condensers and thermofield processes reactors. These processes also contribute greatly to the heating and air-conditioning of buildings. The way airplanes and rockets operate is based on fluid flow, heat transfer and chemical interactions. Heat transfer is often the limiting factor in designing electric machines and circuits (Sparrow and Bahrami, 1980; Sparrow and Azevedo, 1985).

One of the most important processes in heat transfer is created by this buoyancy force. These processes, known as free convection heat transfer, have many applications in industry. For example, they are widely used in air conditioning systems, power transfer transformers, nuclear reactors (melt cooling flow), electronics industry, meteorology, etc. To display the high capacity of this type of heat transfer in industrial applications, one can refer to the cooling tower of the 2,000 MW Shahid Rajaei Power Plant in Qazvin. where water cooling used in the cycle of this large power plant is performed by four cooling towers of more than one hundred

meters in height and under the influence of the free convection transfer phenomenon (Shokouhmand and Hesami, 1993; Levy, 1971; Anand et al., 1992; Bejan and Sciubba, 1992).

The application of heat transfer principles is of high importance in designing specific engineering equipment and the application of heat transfer principles is aimed at heat transfer in designing and achieving the goal of production development for economic profitability. In reality, recognizing the type of converter based on the fluids it passes through has an important role in designing and calculating heat converters economically.

Many researches have been done on increased heat transfer, but most of the work done is experimental in nature because of the complex nature of the flow structure created. In this chapter, previous works in different fields will be described separately (Morrone et al., 1997; Onur and Aktaş, 1998).

In 2004, Das and Dalal (Fu and Huang, 2006) investigated a numerical study of slow free convection in a sloped enclosure with three flat walls and a wavy vertical wall. The operating fluid in this research was air. The variable parameters in their study included Rayleigh number, enclosure's placement angle, change in amplitude to wavelength ratio and change in the number of wavy wall waves from one to three waves. The boundary conditions were in the form of three walls (including a vertical wavy wall) at a fixed cold temperature and an upper wall temperature of a sine function. The findings of their work can be stated as follows:

In all types of wavy plates (plates including one, two and three waves), the maximum mean Nusselt value is at a 300-degree angle.

In small Rayleigh, the mean Nusselt value can be increased by increasing the amplitude.

In large Rayleigh, increasing the sine wave amplitude causes the mean Nusselt value to fall.

As the wave amplitude increases, the heat transfer in the three-wave wall decreases relative to the one- and two-wave wall. In 2006, Ajlut et al. (2002) performed a numerical study of free convection on an enclosure with a wavy wall. The vertical wavy, the opposite wall and the adiabatic vertical walls formed their boundary conditions at fixed hot temperature and fixed cold temperatures respectively. The operating fluid in this study was air and the studies performed in the range of Rayleigh number ranging from 1^9 to 10^{12}. The findings revealed that in contrast to the smooth flow of the enclosure, the presence of a wavy wall increases the local Nusselt value at all angles of the chamber as well as at all Rayleigh numbers under the influence of the hot wavy wall. Besides, a linear relationship was noted between the local Nusselt number and the Rayleigh number. The angle at which the lowest local Nusselt number was seen was reported to be 144 degrees.

The study of free convection heat transfer method is of great importance in many industrial fields and natural processes. Free convection in many cases where heat transfer is not feasible in any other way, restricts heat transfer. Under such circumstances, it is key to increase the heat transfer rate by free convection method to increase the safety factor. The free convection heat transfer process over vertical plates is observed in industrial applications. One of the most important areas where free convection heat transfer occurs from over the plates is the electronic boards inside the computer parts.

The heat dissipated from such electronic circuits has a great impact on their performance. In other applications where the heated plates are smooth, it is necessary to raise the heat dissipation rate to reach the intended temperature level. A common way for this is to add vanes to the plates to increase the heat transfer rate. Included in the heat transfer process by free convection is the condenser of home refrigerators. In such systems, the condenser pipes can be modeled as an uneven vertical plate onto which heat is transferred via free convection.

In many cases, the heat converting plate stands against another plate where heat transfer occurs in one channel.

In these cases, the front panel will have a great impact on the heat transfer rate from the main plate, and the distance between the two plates increases or decreases the heat transfer rate from the main plate. In this study, attempts were made to investigate the free convection heat transfer from over a vane in the vicinity of adiabatic plates.

Materials and Methods

Problem geometry

To model the problem, a two-dimensional problem schema is considered as an element of the above converters.

For a reference mode, a mode introduced by Mr. Sedaghat et al. (2015) and studied in the laboratory is taken into account. The 3D scheme of the problem and the effective parameters are seen in Figure 1:

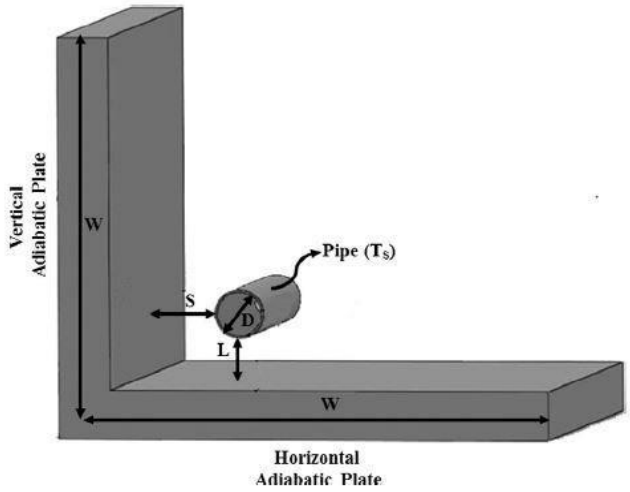

Figure 1: Three-dimensional scheme of a pipe near two adiabatic walls

According to Figure 1:

S: Distance of the cylinder from the vertical wall

L: Distance of the cylinder from the horizontal wall

D: Diameter of the cylinder

TS: Temperature of the outer surface of the cylinder

W: The length of horizontal and vertical walls

The calculation range for this project is a square of 1320 mm in diameter. A cylinder with a diameter of 80 mm is positioned in the lower left corner at a distance of 40 mm from the vertical wall and also at a distance of 80 mm from the horizontal wall. These conditions are in line with the S/D = ½ and L/D = 1 state, tested experimentally in the article (Aounallah et al., 2006) with the relevant results reported.

Boundary conditions

Boundary conditions are summarized in Table 1.

Table 1: Boundary conditions of the problem

Boundary condition name	Conditions imposed
Cylinder	It has an outer surface temperature of 13 ° C
Vertical side wall	Adiabatic
Horizontal side wall	Adiabatic
Far vertical and horizontal walls	Pressure outlet

Network production

Producing a proper grid is one of the most important parts of a numerical solution, as an unsuitable network is associated with divergence of the solution trend and even a wrong answer. As known, to mesh this range,

we first select each individual edge and network it, so that the areas of greater computational importance yield a finer networking. To have a proper focus and to create a proper connection among the mesh of these small volumes, an unorganized mesh designed for this purpose is used. For a higher computational accuracy, approximately the number of 7,500 to 8,500 meshes is used for the entire computational range. This change in the number of networks is due to the change in volume in different stages of the research. This is while that for larger volumes, the number of networks increases also. Because of the complexity of the flow near the obstacles, a finer network is used.

Numerical solution of governing equations

After defining the geometry of the problem and its networking by Gambit 2.3.16 software, the numerical solution of equations governing the problem in the computational range was addressed by ANSYS-Fluent 17 software via the finite volume method. After defining the boundary conditions and selecting the air (=Pr = 0.71) of fixed properties as the operating fluid, (Sedaghat et al., 2015) the solvent is implicitly selected on the basis of pressure and steady flow.

The discretization of convection and energy terms due to higher accuracy is performed using the second-order method, and the SIMPLEC algorithm is used to make velocity and pressure be attached. Laminar model was used for the laminar flow range.

Governing equations

As noted, because of the low velocity of the fluid flow and the nature of the free convection, the flow occurs slowly. Since the velocity is slow the Mach number is lower, air is considered as an incompressible fluid with fixed physical properties. The flow is assumed to have been two-dimensional, stable and without loss of viscosity. The equations governing this flow, including mass conservation and the magnitude of motion and energy (Levy, 1971; Onur and Aktaş, 1998; Turk and Junkhan, 1986), are stated as follows:

Mass conservation equation:

$$\frac{\partial u}{\partial x} + \frac{\partial v}{\partial y} = 0 \tag{1}$$

Momentum equation:

$$u\frac{\partial u}{\partial x} + v\frac{\partial u}{\partial y} = g\beta(T - T_\infty) + v\frac{\partial^2 u}{\partial y^2} \tag{2}$$

Energy equation

$$u\frac{\partial T}{\partial x} + v\frac{\partial T}{\partial y} = \alpha\frac{\partial^2 T}{\partial y^2} \tag{3}$$

Where v and α represent the kinematic viscosity and the heat dissipation coefficient of air, respectively.

Because the governing equations are elliptical in spatial coordinates, a boundary condition is required for all the borders of the computational range.

The heat transfer coefficient is defined using Newton's Convective heat transfer as follows:

$$h = \frac{Q}{A \cdot \Delta T} \tag{4}$$

Where Q is the amount of heat transferred and A is the surface area onto which the heat is transferred in a convective way, ΔT is the discrepancy between the surface temperature and the temperature of the fluid flow. The Nusselt number is a dimensionless number which, in heat transfer, indicates the ratio of heat transferred through convection to heat transferred through conduction at the system's boundary and is stated as follows:

$$\mathcal{N}u = \frac{hH}{k} \tag{5}$$

Independence of the solution depends on the number of elements

To achieve acceptable results, we need to first investigate the networking independence. By networking independence, it is meant that no significant change is made in the answer as the number of elements rises. To do this, we first guess an initial network with a relatively small number of elements. Then, by reducing the distance between the elements and comparing the answers, we will perform the best networking by trial and error.

Initial networking starts at a distance of 30 mm from the input wall and it is networked based on the initial Ansys-Mesh presumption. As well, the total number of elements is 118. However, as the appearance of the mesh shows, no acceptable results will be made using this mesh. Therefore, we increase the number of points to yield a better networking.

In the next stage, we solve the flow field and compare the results with the results from the testing. This networking is not acceptable because of the substantial differences. Therefore, we make the networking finer and in addition, we use several finer layers of square elements near the wall and to better simulate the boundary layer. To reduce the computational cost and to avoid increasing the rounding error, triangular networking is outside the boundary layer. As the elements become finer and at the same time the number of layers of square elements increases with then the answers being compared, finally the vertical and horizontal adiabatic walls are divided into 150 parts with a factor of 4^{19} and the cylinder is also divided into 100 parts. Also, 12 swelling layers with an initial thickness of 1 mm and a growth factor of 1.1 are responsible for simulating the created boundary layer. This part is divided by a square mesh. Thus, 6331 nodes and 7431 elements with 12 swelling layers are formed. After the flow field is solved, an acceptable answer is obtained. To better reveal the number of layers and the shape of the elements, a close-rage view of this networking is illustrated in Figure 2. By making the elements finer and increasing the number to 9756, no noticeable change is seen in the answer. Therefore, to reduce the computational cost, the number of elements 7431 seems reasonable.

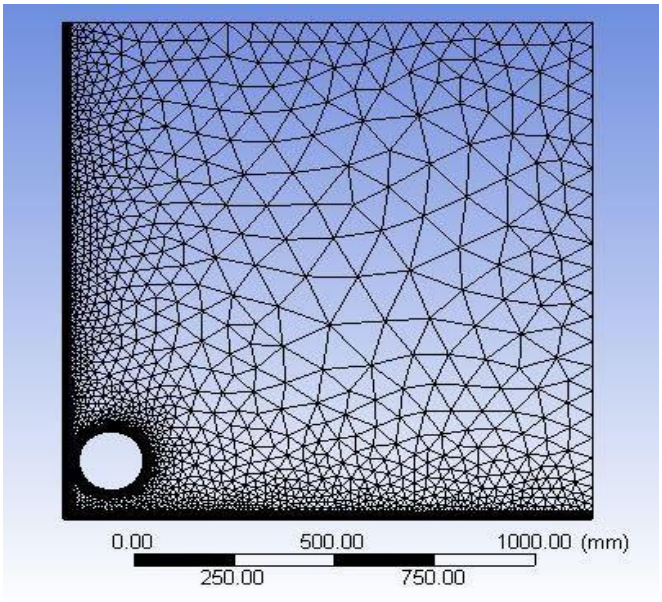

Figure 2: Final meshing

Finally, the effect of the number of elements on the results and the temperature meter in the cylindrical range are also illustrated in Figure 3. As shown no change was seen in the results for elements greater than 8000. Therefore, to reduce the computation time, this number of elements is used for different geometries.

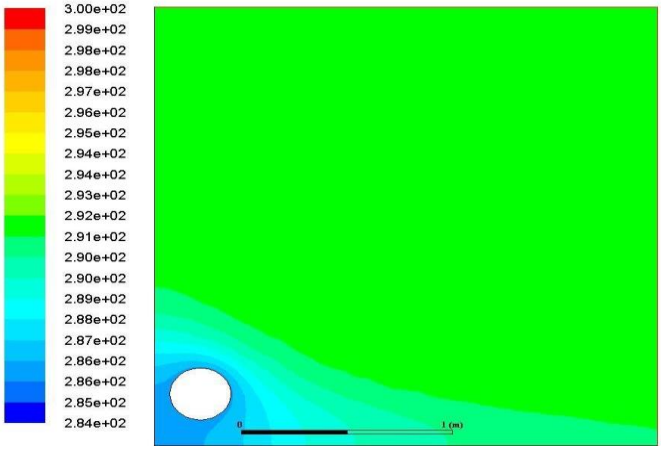

Figure 3: Temperature meter in the cylindrical range

Validating the code used

Considering the fact that the geometry of the problem is the same as the model used by Sedaghat et al. to validate the code in the slow flow, the results were compared with the reported results for inside-enclosure flow.

As reported in the article, the Nusselt number around the cylinder is 12.618. Calculating the weight average of the Nusselt number of the cylinder in this simulation is12.923. By comparing these two numbers as well as the temperature and flow function meters, it becomes clear that the obtained results enjoy an acceptable accuracy.

Results

Investigating the optimal position of the vanes/blades

After the optimal shape and size were obtained from the introduced models, it is time to determine the optimal position of the vane. Thus, the initial position of the vane, placed in the right corner of the cylinder, is rotated by 30 degrees, and after the flow field solution is networked, the mean Nusselt number is calculated. This process is repeated until the blade reaches its original position. In other words, it is rotated 360 degrees. Then, the optimal position of the vane is obtained. In this section, to save time, only the velocity vectors and the Nusselt number diagram for each mode are illustrated.

In this step, we rotate the vane by 30 degrees in a positive trigonometric direction (anti-clockwise). After the flow field is solved, the velocity vectors can be observed in Figure 4a.

The rotation of the placed vane changes the flow structuring around the cylinder and increases turbulence. Due to the presence of a vane on the right wing of the cylinder, the current turbulence increases and as a result the Nusselt number rises also (Figure 5a).

By investigating the results obtained from numerical modeling and comparing them with the unobstructed state, one can conclude that by placing the vane in a triangular form at a 30-degree angle to the horizon, the mean Nusselt number rose to 0.133 after 0.96%.

Then we rotate the same vane again by 30 degrees in a positive trigonometric direction (anti-clockwise) so that the vane will be at a 60-degree angle to the horizon. After the flow field is solved, the velocity vectors in Figure 4 can be seen.

The rotation of the placed vane changes the flow structuring around the cylinder and increases turbulence. Because of the presence of a vane on the right wing of the cylinder, the current turbulence increases and as a result the Nusselt number also rises (Figure 5 b).

By investigating the results obtained from numerical modeling and comparing them with the unobstructed state, one can conclude that by placing the vane in a triangular form at a 60-degree angle to the horizon, the mean Nusselt number rose to 13.033 after a rise of 0.85%.

In the next step, we rotate the same vane again by 30 degrees in a positive trigonometric direction (anti-clockwise). Thus, the vane will be at an 120-degree angle to the horizon. After the flow field was solved, the velocity vectors are seen in figure 4c. The rotation of the placed vane changes the flow structuring around the cylinder and increases turbulence. Because of the presence of the vane on the wing of the cylinder, the current turbulence increases and as a result, the Nusselt number also rises (Figure 5 c).

By investigating the results obtained from numerical modeling and comparing them with the unobstructed state, one can conclude that by placing the blade in a triangular shape at a 120-degree angle to the horizon, the mean Nusselt number rose to 1.484 after 1.244%.

In the next step, we rotate the same vane again by 30 degrees in a positive trigonometric direction (anti-clockwise). Thus, the vane will be at an angle of 150 degrees to the horizon. After the flow field was solved, the velocity vectors can be seen in figure 4d. As seen, the rotation of the placed vane changes the flow structuring around the cylinder and causes the turbulence to rise. Because of the presence of the vane on the wing of the cylinder, the current turbulence increases and as a result, the Nusselt number also rises (Figure 5d).

By investigating the results obtained from numerical modeling and comparing them with the vane-less state, one can conclude that by placing the vane in a triangular shape at an angle of 150 degrees to the horizon, the mean Nusselt number increases to 13,044 after 1.11.

By investigating the results obtained from numerical modeling and comparing them with the vane-less state, one can conclude that by placing the vane in a triangular shape at a 180-degree angle to the horizon, the mean Nusselt number increases to 13.0638 after 1.0897 percent.

In the next step, we rotate the same vane again by 30 degrees in a positive trigonometric direction (anti-clockwise). Thus, the vane will be at an angle of 120 degrees to the horizon. After the flow field is solved, the velocity vectors can be seen in figure 4e. The rotation of the placed blade changes the flow structuring around the cylinder and causes the turbulence to rise. Because of the presence of the vane on the wing of the cylinder,

the turbulence of the current rises and as a result, the Nusselt number also rises (Figure 5e). By investigating the results obtained from numerical modeling and comparing them with the vane-less state, one can conclude that by placing the vane in a triangular shape at an angle of 210 degrees to the horizon, the mean Nusselt number rises to 13.0636 after 1.088%. In the next step, we rotate the same vane again by 30 degrees in a positive trigonometric direction (anti-clockwise). Thus, the vane will be at an angle of 330 degrees to the horizon. After the flow field is solved, the velocity vectors are seen in figure 4f. The rotation of the placed blade changes the flow structuring around the cylinder and increases the turbulence. Because of the presence of the vane on the wing of the cylinder, the turbulence of the current rises and as a result, the Nusselt number also rises (Figure 5e).

By investigating the results obtained from numerical modeling and comparing them with the vane-less state, it is concluded that by placing the blade in triangular shape at an angle of 330 degrees to the horizon, the mean Nusselt number increases to 13.0859 after 1.02606.

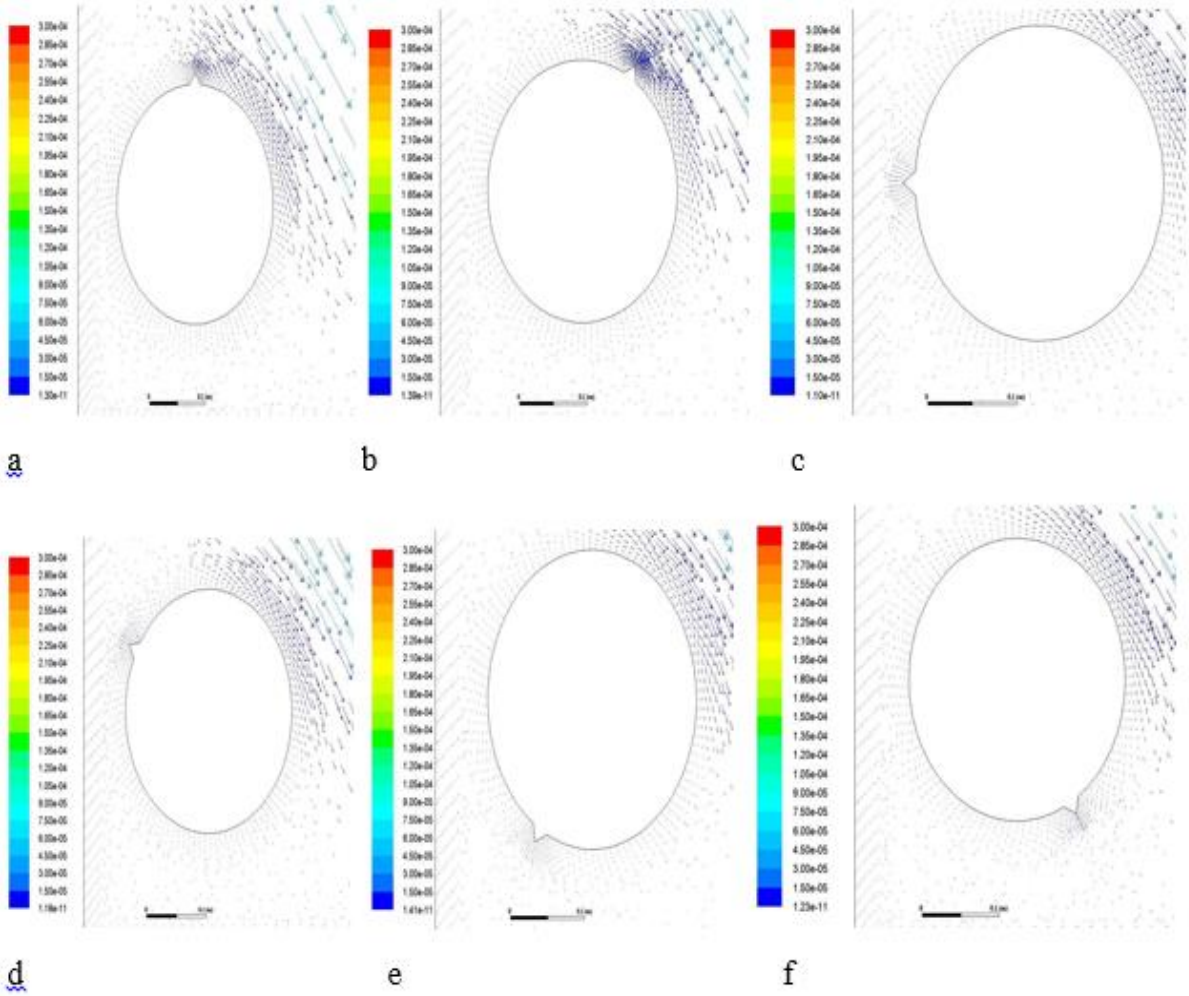

Figure 4: Velocity vector around the cylinder after the vane is placed

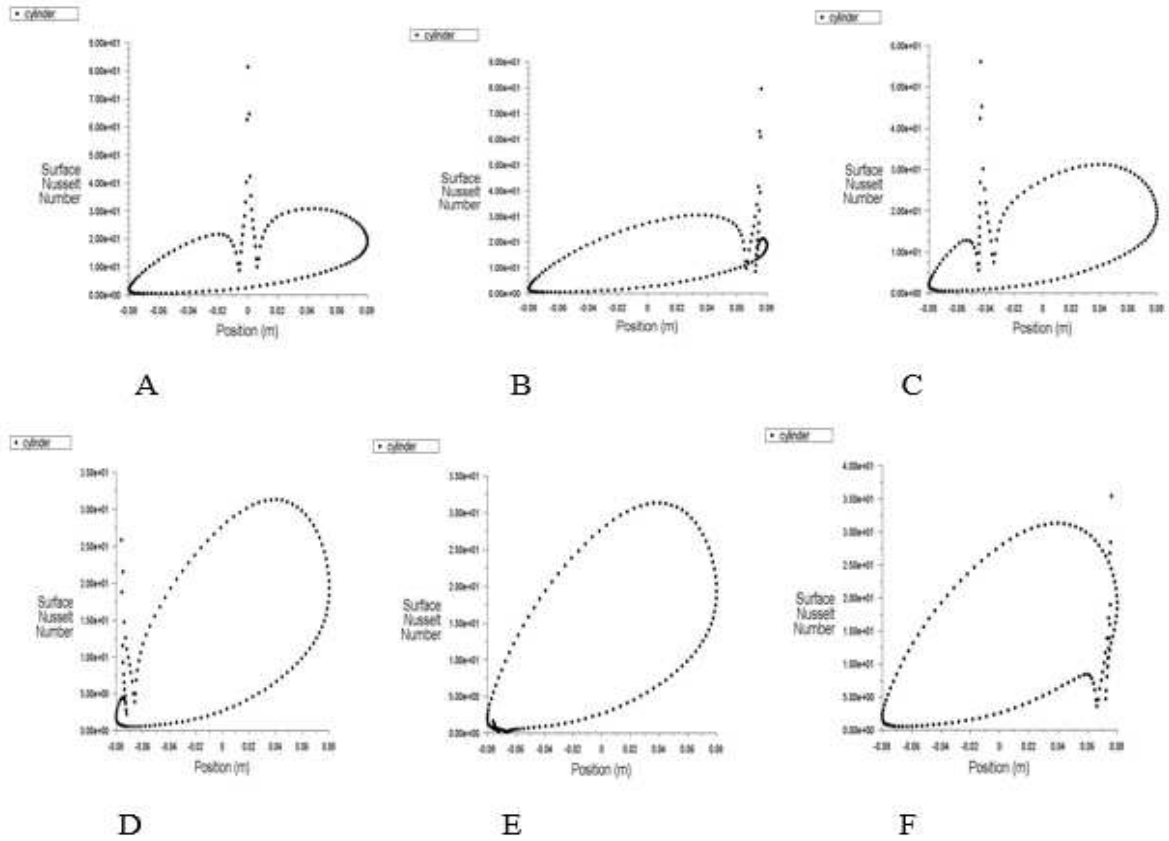

Figure 5: Changes in the Nusselt number of cylinders

After this step, by increasing the position of the vane by 30 degrees, the same zero-degree position is obtained, which will not be repeated as discussed in the previous section. To better understand the results, the mean Nusselt number of each position and its rise compared to the baseline is provided in Table 2.

Table 2: Different positions of the triangular vane angles studied

Angle	Mean Nusselt number	Percentage of increase to the Nusselt number compared to the base model
0	13.135	1.640485955
30	13.012997	0.696409502
60	13.033286	0.853408651
90	13.087747	1.274835564
120	13.083802	1.244308597
150	13.066466	1.11016018
180	13.063825	1.089723748
210	13.063603	1.088005881
240	13.062094	1.076329026
270	13.066729	1.112195311
300	13.066082	1.107188733
330	13.085909	1.260612861

Also, the percentage of change to the mean Nusselt number in terms of a function of the position of the triangular vane around the cylinder is plotted in Figure 6

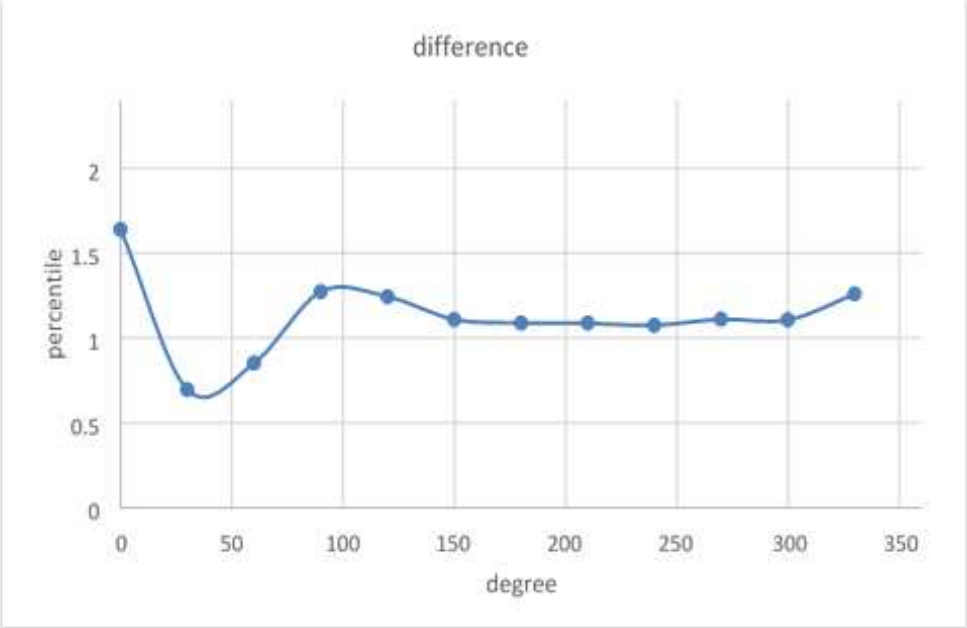

Figure 6: Percentage of the mean Nusselt number variation as a function of the triangular vane angle around the cylinder

Investigating Table 2 and Figure 6, it becomes clear that the vane in the zero-degree position will have the highest efficiency and can improve the heat transfer performance of the cylinder by 1.64%. It also descends to the lowest efficiency at an angle of 30 degrees, and in this position, we see only a 0.7% rise in free convection heat transfer.

Conclusion

In the present study, we studied the free convection heat transfer around the cold cylinder near two adiabatic walls. The results from modeling the studied geometry were found to be in good agreement with the experimental results, indicating the accuracy of the modeling.

In this study, in order to optimize the free convection heat transfer around the cylinder, vanes were installed around the cylinder to improve the heat transfer process. The geometry (shape and size) of these vanes and their position are the items investigated in this study. For this, first three geometric shapes with low manufacturing costs were considered to play the role of the vane. Then each of them was examined in two different sizes, small and large, in the right corner of the cylinder. Of course, in order to find the optimal state, we must consider an increased mean Nusselt number, which is a criterion for evaluating the performance of free convection heat transfer. Therefore, the model with most percentage in heat transfer was considered as the optimal mode. After the best shape and size of the vane was found in a fixed place next to the cylinder, the position of the vane was examined. Thus, the blade was rotated 30 degrees in a positive trigonometric direction each time (anti-clockwise) to reach its original position. For each of these 12 possible states, the mean Nusselt number was calculated and reported in the corresponding diagram. This again showed the best position with the highest increase in the free convection heat transfer compared to the baseline state. The general results obtained in this study are as follows:

1- The geometry of the studied vanes are: triangle, rectangle and quasi-rectangle. It should be noted that each of these shapes is modeled in different dimensions.

2- The small triangular obstacle creates the largest increase in the mean Nusselt number. Then there are large triangular vanes and small square blades.
3- Large rectangular vane is least improved in heat transfer performance compared to other vanes.
4- The best place for the vane is between -0.3 to +0.3 degrees (to the right of the cylinder).

Reference

1. Adjlout, L., Imine, O., Azzi, A., & Belkadi, M. (2002). Laminar natural convection in an inclined cavity with a wavy wall. *International Journal of Heat and Mass Transfer*, *45*(10), 2141-2152.
2. Anand, N. K., Kim, S. H., & Fletcher, L. S. (1992). The effect of plate spacing on free convection between heated parallel plates. *Journal of Heat Transfer (Transactions of the ASME (American Society of Mechanical Engineers), Series C);(United States)*, *114*(2).
3. Aounallah, M., Addad, Y., Benhamadouche, S., Imine, O., Adjlout, L., & Laurence, D. (2006). Numerical investigation of turbulent natural convection in an inclined square cavity with a hot wavy wall. *International Journal of Heat and Mass Transfer*, 47: 1016-1027.
4. Bejan, A., & Sciubba, E. (1992). The optimal spacing of parallel plates cooled by forced convection. *International Journal of Heat and Mass Transfer*, *35*(12), 3259-3264.
5. Fu, W. S., & Huang, C. P. (2006). Effects of a vibrational heat surface on natural convection in a vertical channel flow. *International Journal of heat and mass transfer*, *49*(7-8), 1340-1349.
6. Gebhart, B., Jaluria, Y., Mahajan, R. L., & Sammakia, B. (1988). Bouyancy-induced flows and transport.-Berlin-Heidelberg.
7. Holman Jack, P., Malekzadeh Translator., & Heshaar, K. (1992). Heat Refining, Maon Pass, Farid Ettaarat, Meta.
8. Levy, E. K. (1971). Optimum plate spacing for natural free convection heat transfer from parallel vertical flat plates.*ASME Journal Heat Transfer*,76: 463-465.
9. Morrone, B., Campo, A., & Manca, O. (1997). Optimum plate separation in vertical parallelplate channels for natural convective flows: incorporation of large spaces at the channel extremes. *International Journal of Heat and Mass Transfer*, *40*(5), 993-1000.
10. Onur, N., & Aktaş, M. K. (1998). An experimental study on the effect of opposing wall on natural convection along an inclined hot plate facing downward. *International communications in heat and mass transfer*, *25*(3), 389-397.
11. Park, H. M., & Chung, O. Y. (1999).Inverse natural convection problem of estinating Wall heat flux using a moving sensor: *International Journal Heat Transfer*, 121: 827-836.
12. Park, H. M., & Jung, W. S. (2001). The Karhunen–Loève Galerkin method for the inverse natural convection problems. *International Journal of Heat and Mass Transfer*, *44*(1), 155-167.
13. Sedaghat, M. H., Yaghoubi, M., & Maghrebi, M. J. (2015). Analysis of natural convection heat transfer from a cylinder enclosed in a corner of two adiabatic walls. *Experimental Thermal and Fluid Science*, *62*, 9-20.
14. Shokouhmand, H., & Hesami, H. (1993). Natural convection heat transfer in vertical flat channel with uniform heat flux and variable thermal property. M. S. Thesis, university of Tehran.
15. Sparrow, E. M., & Azevedo, L. F. A. (1985). Vertical-channel natural convection spanning between the fully-developed limit and the single-plate boundary-layer limit. *International Journal of Heat and Mass Transfer*, *28*(10), 1847-1857.
16. Sparrow, E. M., & Bahrami, P. A. (1980). Experiment on natural convection from vertical parallel plates with either open or closed edges. *ASME Journal Heat Transfer*,106: 221-227.
17. Turk, A. Y. & Junkhan, G. H. (1986). Heat transfer enhancement downstream of vortex generators on flat plate, Proc. *8th International Heat Transfer Conf, Heat Transfer (Hemisphere, New York)*, 6: 2903-2908.